JOURNAL OF MATERIALS SCIENCE 31 (1996) 2687–2692

Mechanical properties of thermosets

Part I *Tensile properties of an anhydride cured epoxy*

A. TCHARKHTCHI*, S. FAIVRE, L. E. ROY, J. P. TROTIGNON, J. VERDU
ENSAM 151, Boulevard de l'Hopital 75013 Paris France

The tensile properties of a DGEBA (diglycidylether of bisphenol A)–norbornene anhydride network ($T_g \approx 130 \pm 5\,^{\circ}C$), were studied in the range (220 K–T_g); 4×10^{-4} to $14 \times 10^{-3}\,s^{-1}$. The viscoelastic spectrum (1 Hz) reveals a low β transition at 220 K. The bulk modulus is practically constant between 200 K and $T_g - 20$ K. The Poisson's ratio increases very slowly until $T_g - 30$ K. Then it increases rapidly to reach its asymptotic value (0.5) near to T_g. The tensile (E) and shear (G) moduli display the classical behaviour linked to viscoelasticity. Plastic yielding occurs at $T \geq 80\,^{\circ}C$, the elongation at yield is almost temperature and strain rate independent ($\varepsilon_Y = 0.035$), whereas the yield stress obeys Kambour's relationship: $\sigma_y = 1.1\,(T_g - T)$ and Eyring's law (activation volume = 914 $cm^3\,mol^{-1}$). Physical ageing at 120 °C strongly affects the yield stress and the ductility. The maximum draw ratio, obtained at $T \geq T_g$, is $\Lambda_{RC} = 1.35$, which seems to be consistent with the network's crosslink density.

1. Introduction

It is often claimed that "thermosets are stiffer than thermoplastics" or "thermoplastics are tougher than thermosets" but such generalizations are derived from considerations of rubbery state properties in which the crosslink density plays a key role. The extension of these generalizations to glassy state properties is, no doubt, abusive. Polystyrene (PS) for instance, is more brittle and stiff than the great majority of epoxy networks of the DGEBA (diglycidylether of bisphenol A) type, crosslinked by diamines, with glass transition temperatures (T_g) higher than PS one (≈ 380 K). Have thermosets specific properties in the glassy state? Despite a relatively abundant literature on their thermomechanical properties [1–8], it is relatively difficult to answer rigorously this question which could be tentatively reformulated as follows: Are the mechanical (especially fracture) properties predictable from the relationships established between these properties and the entanglement density in linear polymers? In other words, can a thermoset be considered as a linear polymer of very high entanglement density? Relatively recent results obtained in both families seem to lead, in this way, to a contradiction. For instance Lemay and Kelley [9] showed that, for a series of epoxies, toughness is an increasing function of the average molecular mass of the network segments M_c.

$$K_{1c} \propto M_c^{1/2} \tag{1}$$

In contrast, Wu [10] showed that, for a very large series of linear polymers, ductility, (sharply linked to toughness), is a decreasing function of the molar mass between entanglements M_e.

It is noteworthy that the higher range of M_c values in the Lemay and Kelley series coincided with the lower range of M_e values in Wu's series and that the nature (entanglements or covalent bonds) of crosslinks do not seem to play a key role in both theories. There are perhaps trivial causes to such a disagreement. For instance, Lemay and Kelley consider an homogeneous set of data in which all the samples undergo fracture in the same kinetic regime (involving presumably devitrification at the crack tip), whereas Wu considers rather the ductile–brittle transition (11).

Anyhow, there is currently, to our knowledge no satisfactory answers to the above questions. Starting from this observation, we decided to study the mechanical properties of a series of thermosets, emphasis being placed on the brittle–ductile transition and relationships between ultimate properties and structure. This first part deals with the study of the tensile properties of an epoxy-anhydride network characterized by a relatively high crosslink density ($M_c \approx 220\,g\,mol^{-1}$), a relatively low local mobility, (as assessed by the intensity of the β transition peak), and a noticeable segment flexibility responsible for a relatively low glass transition temperature ($T_g \approx 130\,^{\circ}C$).

2. Experimental procedure

2.1. Materials

The network was based on a DGEBA diepoxide ($M = 383\,g\,mol^{-1}$) and norbornene anhydride as a curing agent. The theoretical structure of the network is shown at the top of the next page:

*To whom all correspondence should be addressed

0022–2461

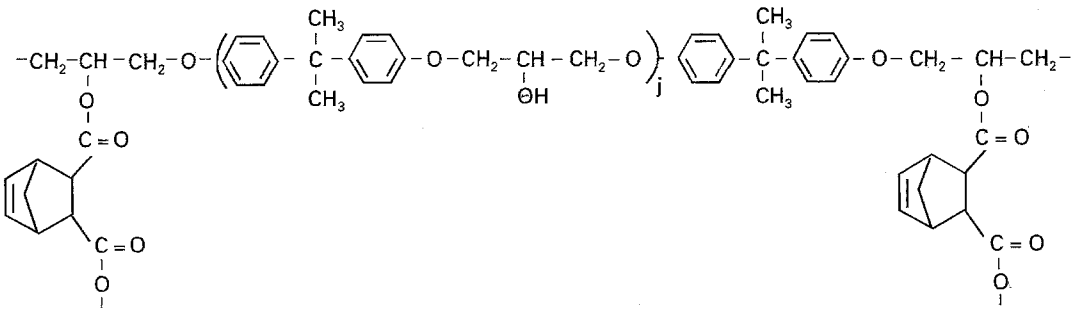

Crosslinking by the internal hydroxyl, (3.75% of the whole DGEBA functionality) is neglected in the calculation of stoichiometric composition. Benzyl dimethyl amine was used as a catalyst. The following cure schedule was used:

(a) Mixing 5 min at 120 °C in oil bath.

(b) Degassing under primary vacuum 10 min at 120 °C.

(c) Casting in a mold cavity having the shape and dimensions of an ISO/1 tensile specimen.

(d) Cure 10 h at 160 °C.

(e) De-molding.

(f) Sample machining in order to adjust the thickness (4 mm) and to eliminate surface defects.

(g) Post cure 30 min at 180 °C.

In these conditions, a supplementary cure treatment would not significantly increase the glass transition temperature (T_g). In order to optimize the network structure, attempts were made with various mixtures differing by the anhydride/epoxide functionality ratio A/E, using the above cure schedule in all cases. The results to be discussed in detail in section 3, lead to an optimum value A/E = 0.86.

2.2. Tensile testing

An Instron 4502, tensile testing machine equipped with a bidimensional extensometer (Instron 25 mm GL) and a ventilated climatic chamber, was used for tensile measurements. Each measurement was made after temperature stabilization, as checked by a temperature sensor on the sample surface. The viscoelastic spectrum was determined in flexural mode, at 1 Hz frequency, using the Polymer Laboratories DMTA viscoanalyser. Differential scanning calorimetry measurements were made using a Perkin Elmer DSC 2 apparatus at a 20 K.min^{-1} scanning rate.

3. Results and discussion

3.1. Optimal network structure

The aim of this preliminary study is to determine the composition of the anhydride-epoxide mixture leading to the maximum crosslink density.

Various samples differing by the A/E functionality ratio were prepared using the previously described cure schedule. The final glass transition temperature was determined by DSC at the inflexion point of the thermogram. Esters and anhydrides can be easily distinguished by FTIR using their characteristic bands at

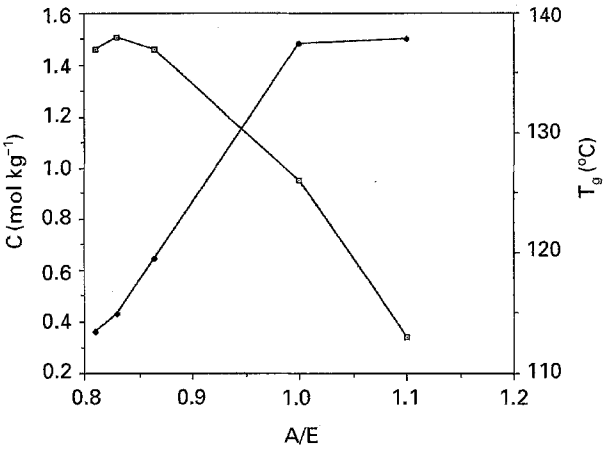

Figure 1 Anhydride concentration (◆) and glass transition temperature (⊡) against stoichiometry ratio A/E.

1740 cm^{-1} and 1780 cm^{-1}. The anhydride concentration determined from the absorbance of this latter band is plotted in Fig. 1 together with T_g, against A/E. The T_g displays a maximum close to A/E = 0.86. For this sample, the residual epoxide concentration determined at 910 cm^{-1} is insignificant.

These results suggest that the maximum crosslink density is obtained for A/E = 0.86 against the 1.0, theoretical value in the case of a pure epoxide-anhydride reaction. It can be reasonably assumed that this is due to the occurrence of an epoxide-epoxide (etherification) reaction [12]. The equilibrated character of the epoxide-anhydride reaction [13] explains the existence of residual anhydride in systems having a noticeable epoxide excess. IR spectra do not reveal the existence of a significant concentration of epoxide or acid (ν = 1710 cm^{-1}) dangling chains. It seems thus reasonable to represent the materials structure as a copolymer of "ether" and "ester" units:

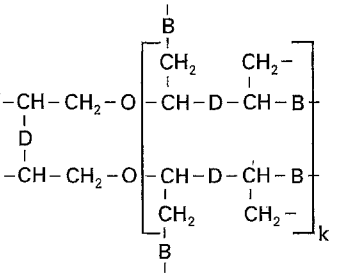

where:

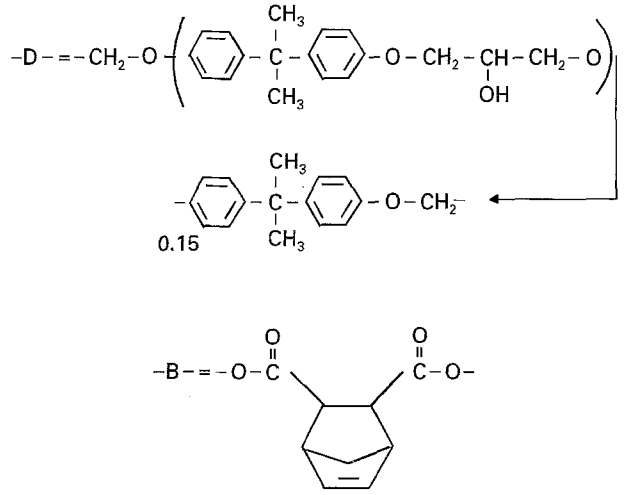

This network contains three types of segments:

$$-D-;\ -CH_2-B-\ \text{and}\ -CH_2-O-$$

These segments are composed of the following statistical units (undeformable skeleton groups separated by rotatable bands):

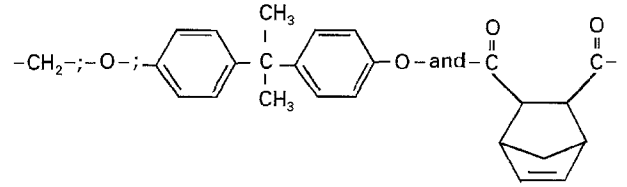

The mode of counting statistical units can carry some ambiguities, but in the case under study, any counting mode would lead to the same conclusions. The three types of network segments have thus the following characteristics:

$N_D = 4.75$; $M_D = 296.6\ g\,mol^{-1}$

$N_{-CH_2-B-} = 4$; $M_{-CH_2-B-} = 194\ g\,mol^{-1}$

$N_{-CH_2-O-} = 2$; $M_{-CH_2-O-} = 30\ g\,mol^{-1}$

Where N_i is the number of statistical units in the segment i of molar mass M_i. The network structure can be deduced from the initial composition, using the above model in which:

$$\frac{B}{D} = \frac{2A}{E} = \frac{4k}{2k+1} \qquad (2)$$

Three hypotheses of network structure are considered:

(i) A/E = 1 (stoichiometric network without etherification): We will arbitrarily choose $k = 1$

(ii) A/E = 0.86 as experimentally found but we will consider that all of the anhydride is reacted. In this case $k \approx 3$.

(iii) A/E = 0.80 It is assumed that for an initial A/E value of 0.86, there is unreacted anhydride as shown by FTIR, so that the A/E value in the network would be 0.80.

The characteristics of the network corresponding to the above hypotheses are listed in Table 1. Two methods for the calculation of M_c were used: M_{c1} is the number average molar weight of the network segments. M_{c2} is the molar weight of the network unit divided by the number of segments. In other words, the mass of crosslinks (–CH–) is taken into account in M_{c2} but not in M_{c1}.

It appears thus reasonable to suppose that we are in the presence of a network having $M_c = 220 \pm 20\ g\,mol^{-1}$, slightly plasticized by a small quantity of unreacted anhydride.

3.2. Transitions

DSC measurements lead to a T_g value of $130 \pm 5\,°C$. A DMTA spectrum, obtained at 1Hz, is presented in Fig. 2. It displays its α peak near to 130 °C, e.g. in good agreement with the DSC data, and a small (compared to amine crosslinked epoxies) secondary peak close to $-50\,°C$.

3.3. Elastic properties

The Young's modulus E and Poisson's ratio ν were determined for four strain rates: $4.54 \times 10^{-4}\,s^{-1}$; $1.44 \times 10^{-3}\,s^{-1}$; $4.54 \times 10^{-3}\,s^{-1}$ and $1.44 \times 10^{-2}\,s^{-1}$ at various temperatures between $-50\,°C$ and T_g. The results are presented in Figs 3 and 4. From E and ν, the shear modulus G and the bulk modulus B were calculated. Their variations with temperature are presented in, respectively, Figs 5 and 6. The results can be summarized as follows:

(i) The bulk modulus is free of viscoelastic effects and is constant until about $T_g - 20\,°C$.

(ii) The Poisson's ratio is almost strain rate independent and increases slowly with temperature ($\nu \approx 0.40$ at $-50\,°C$ and 0.41–0.42 at $T_g - 30\,°C$. Above this limit, e.g. in the glass transition regime, it increases rapidly to reach a value of 0.5, characteristic of a rubber, in close vicinity of T_g.

(iii) Both shear and Young's moduli display the expected viscoelastic behaviour in both regions of β and α transitions. Concerning the latter, the shift due to a shear rate variation begins to be observable at $T_g - 100\,°C$, e.g. far below the temperature at which B and ν become rate sensitive.

3.4. Yield

The shape of tensile curves at various temperatures and a $2.88 \times 10^{-3}\,s^{-1}$ strain rate is shown in Fig. 7. Plastic yielding occurs only above 60 °C. The yield strain: $\varepsilon_y = 0.033 \pm 0.002$ is almost independent of temperature, whereas the yield stress decreases almost linearly with temperature (Fig. 8). For instance, for $\varepsilon = 2.88 \times 10^{-3}\,s^{-1}$:

$$\sigma_y \approx 447 - 1.1\,T \qquad (3)$$

where σ_y is in MPa and T in K.

According to this relationship, $\sigma_y = 0$ for $T = 406$ K e.g. for $T = T_g$ within experimental scatter. Thus, as

TABLE I Characteristics of the networks according to three hypotheses

Characteristic	Hypothesis (i)	Hypothesis (ii)	Hypothesis (iii)
Number of segments –D–	2	7	5
Number of segments $-CH_2-B-$	4	12	8
Number of segments $-CH_2-O-$	0	2	2
M_{c1} (g mol^{-1})	228	213	206
M_{c2} (g mol^{-1})	237	221	215

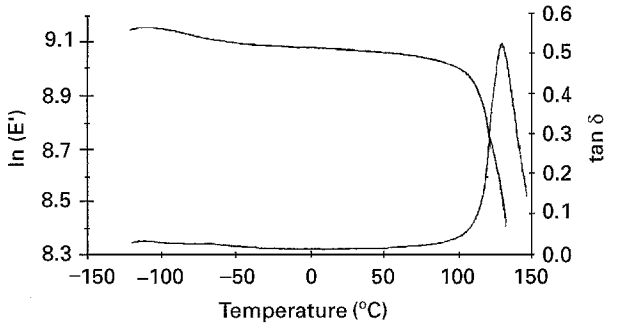

Figure 2 DMTA spectrum at 1 Hz.

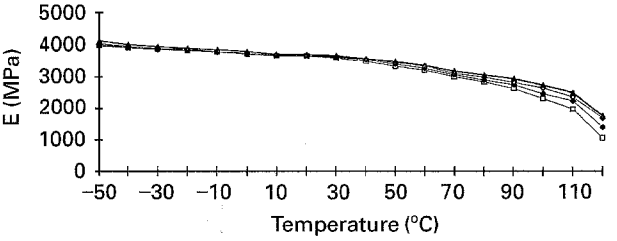

Figure 3 Young's modulus against temperature at $4.54 \times 10^{-4}\,s^{-1}$ (□); $1.44 \times 10^{-3}\,s^{-1}$ (◆); $4.54 \times 10^{-3}\,s^{-1}$ (◇) and $1.44 \times 10^{-2}\,s^{-1}$ (△) strain rate.

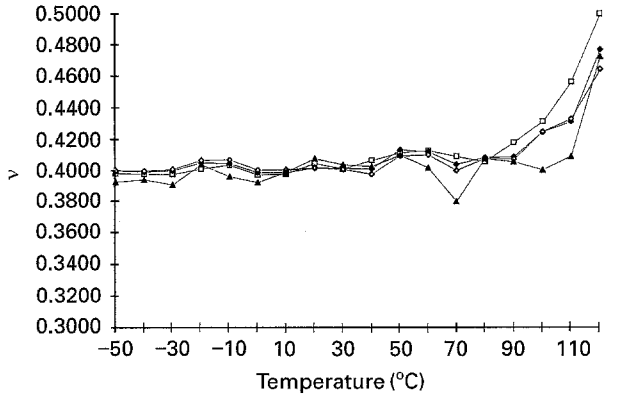

Figure 4 Poisson's ratio against temperature at $4.54 \times 10^{-4}\,s^{-1}$ (□); $1.44 \times 10^{-3}\,s^{-1}$ (◆); $4.54 \times 10^{-3}\,s^{-1}$ (◇) and $1.44 \times 10^{-2}\,s^{-1}$ (▲) strain rate.

derived from Kambour's relationship [14]:

$$\sigma_y = 1.1\,(T_g - T) \tag{4}$$

Strain rate effects have been studied at 100 °C. They seem to obey Eyring's law (Fig. 9). The slope of the straight-line is (R/V) = 9100. From the measurements made at a fixed strain rate and various temperatures,

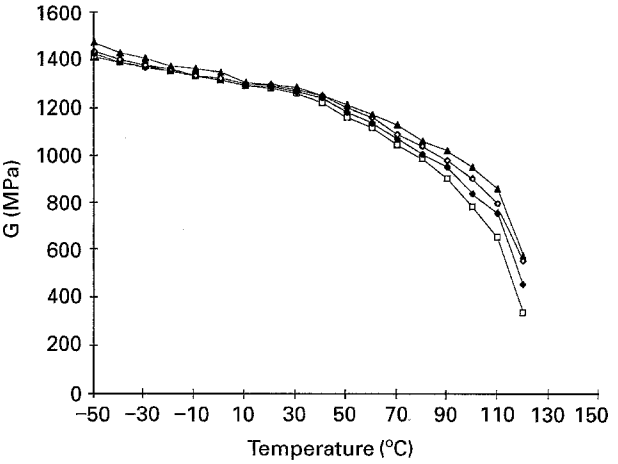

Figure 5 Shear modulus against temperature at $4.54 \times 10^{-4}\,s^{-1}$ (□); $1.44 \times 10^{-3}\,s^{-1}$ (◆); $4.54 \times 10^{-3}\,s^{-1}$ (◇) and $1.44 \times 10^{-2}\,s^{-1}$ (▲) strain rate.

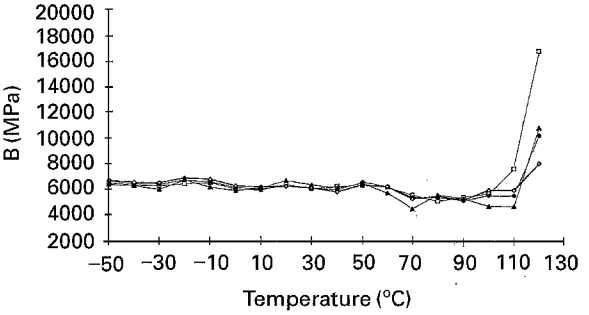

Figure 6 Bulk modulus against temperature at $4.54 \times 10^{-4}\,s^{-1}$ (□); $1.44 \times 10^{-3}\,s^{-1}$ (◆); $4.54 \times 10^{-3}\,s^{-1}$ (◇) and $1.44 \times 10^{-2}\,s^{-1}$ (▲) strain rate.

we obtained:

$$\dot{\varepsilon} = \dot{\varepsilon}_0 \exp -\frac{Q - V\sigma}{PT} \tag{5}$$

with $Q = 393\ \text{kJ.mol}^{-1}$ and $V = 914\ \text{cm}^3\,\text{mol}^{-1}$.

3.5. Ductile–brittle transition

The maximum stress σ_M and the ultimate elongation ε_R determined at a $2.88 \times 10^{-3}\,s^{-1}$ strain rate were plotted against temperature in Fig. 8. For the strain rate under study, the ductile–brittle transition appears clearly as a discontinuity in both curves at a temperature T_B between 60 and 80 °C. For $T < T_B$, σ_M is the stress at (brittle) rupture, almost independent of temperature: $\sigma_M \approx 40$ MPa. For $T \geq T_B$, $\sigma_M = \sigma_Y$ (yield stress). σ_Y decreases linearly with temperature. ε_R varies abruptly from about 2.5×10^{-2} at 60 °C to

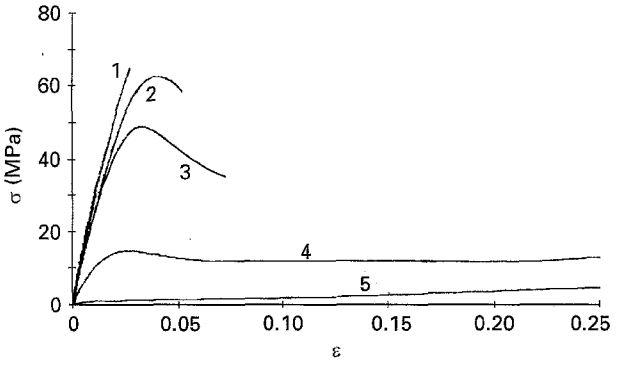

Figure 7 Shape of tensile curves at $2.88 \times 10^{-3}\,s^{-1}$ strain rate for various temperatures: 1 (60 °C), 2 (80 °C); 3 (100 °C); 4 (120 °C) and 5 (140 °C).

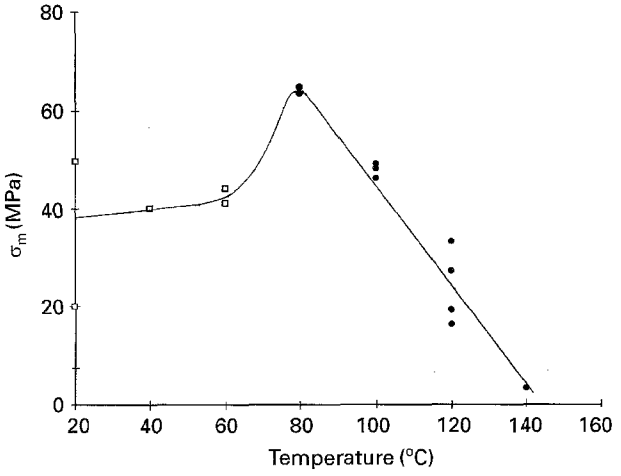

Figure 8 Maximum stress against temperature. (□) brittle rupture; (●) yield.

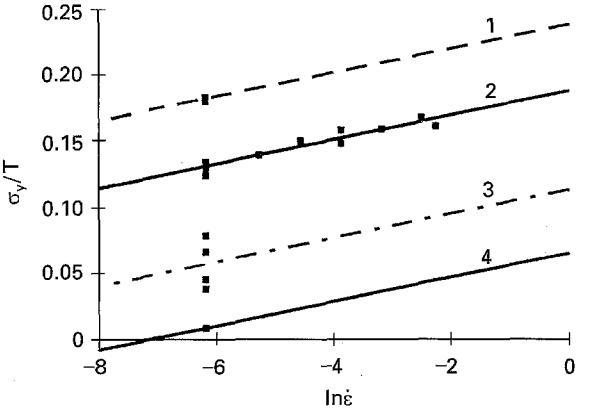

Figure 9 Eyring plot for the yield point at (1) 80 °C, (2) 100 °C, (3) 120 °C and (4) 140 °C.

5×10^{-2} at 80 °C. Thus $T_B \approx T_g - 60$ K. T_B does not correspond to a transition observable by viscoelastic measurements.

3.6. Physical ageing effects

Tensile curves corresponding to increasing times of ageing at 120 °C (tensile testing at the same temperature) are presented in Fig. 10. The yield stress varies

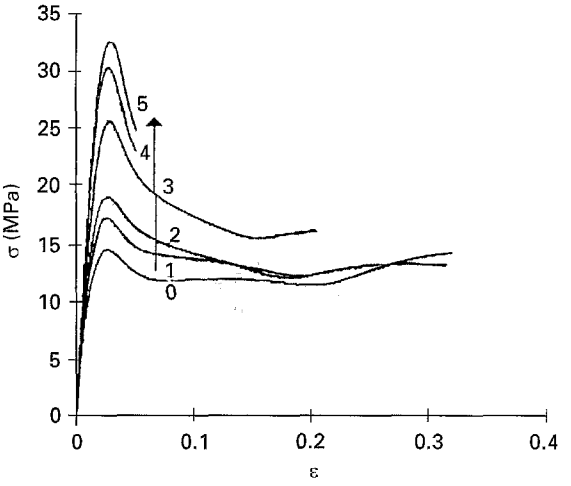

Figure 10 Effect of physical ageing at 120 °C (T_g–10) on tensile curves: 0 (140 °C); 1 (120 °C); 2 (100 °C); 3 (180 °C); 4 (60 °C) and 5 (20 °C).

from 15–32 MPa whereas the elongation at rupture is divided by a factor of about 5. Ageing effects are completely suppressed by heating far above T_g (180 °C), followed by quenching to ambient temperature and reheating at 120 °C. This behaviour can be, no doubt, attributed to physical ageing [15]. It indicates that ductility may be regarded, to a large extent, as a non equilibrium property.

3.7. Ultimate behaviour in the glass transition domain

When the polymer is in its rubbery state, its ultimate elongation ε_R reaches an asymptotic value almost independent of temperature and strain rate: $\varepsilon_{RR} = 0.35$ corresponding to a draw ratio $\Lambda_{RR} = 1.35$. This value calls for the following comments:

(i) It is obvious that the brittleness observed at ambient temperature is not directly linked to the extensional capability of the network since the ultimate elongation is at least ten times lower than the maximum possible elongation observed in the rubbery state.

(ii) Does the value of Λ_{RR} correspond to the maximum extension of network segments? Methods to estimate Λ_{RR} from chain statistics in linear polymers are well known [16, 17] but they are difficult to apply to thermosets owing to the shortness of chains (statistics are questionable) and their diversity. It seemed to us interesting to try to appreciate the extensibility of the longest network chain (–D–) by comparing the end to end separation r_0 in the most compact and the most extended conformation (Fig. 11). The ratio is about 2.5. Indeed the equilibrium (unstressed) conformation is expected to correspond to an intermediary value of r_0. Furthermore, in a network containing various types of chains, the shortest ones limit the extensibility as shown in model rubbers [18]. It seems thus not unreasonable to suppose that Λ_{RR} corresponds well to the maximum extensibility of the network under study at the molecular scale (provided that the classical hypothesis of affine deformations is valid, at least in a first approximation.

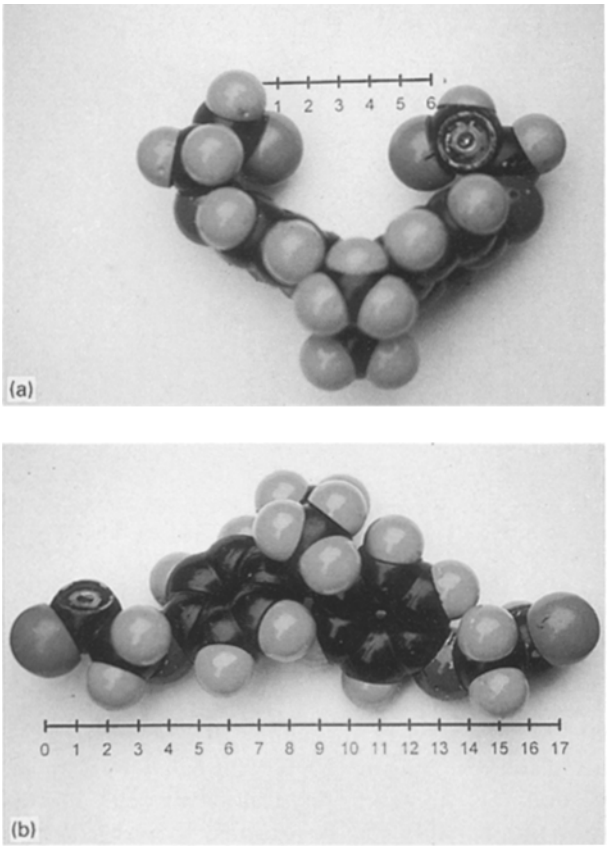

Figure 11 Shortest and longest conformations of the segment –D–.

4. Conclusions

The network under study is characterized by a low local mobility as assessed by the intensity of its β dissipation peak at ≈220 K (1 Hz). Most of its tensile properties are very similar to those of linear polymers characterized also by a low local mobility such as polystyrene (PS) or polymethacrylates (PM). Their tensile modulus at ambient temperature is relatively high ($E = 3.2$ GPa against 2.4–2.8 GPa for linear polymers of high local mobility such as polycarbonate or polysulfones and for networks such as amine crosslinked difunctional epoxies [5]. As PS or PM, the network under study is ductile and presumably undergoes physical ageing at a significant rate [15], in a short temperature range below T_g. The lowest limit of this range, T_B, does not correspond to the β transition as for polymers of high local mobility such as polycarbonate, polysulfones or PVC. $T_B/T_g \approx 0.85$ for the anhydride cured epoxy, a value which is comparable with PS or PMMA ones [11]. In the ductile domain, the yield stress is a linear function of the temperature as already observed for amine crosslinked epoxies [3] and for crazing of linear polymers [14]. Finally, differences appear only at quantitative level: The Poisson's ratio appears higher for the network (0.40) than for PS or PMMA ($\nu \leq 0.37$ at ambient temperature), and, as expected, the maximum extension ratio, presumably linked to the length of network chains, is limited to 1.35 against more than 5 in linear polymers such as PS or PMMA, far above their entanglement limit.

References

1. D. H. KAELBLE, in "Epoxy Resins" edited by C. A. May and Y. Tanaka (Marcel Dekker, New York, 1973) p. 330.
2. S. C. MISRA, J. A. MANSON and L. H. SPERING, *Adv. Chem. Ser.* **114** (1979) 137.
3. V. B. GUPTA, L. T. DRZAL and C. Y. C. LEE, *Polym. Eng. Sci.* **17** (1977) 837.
4. R. J. MORGAN, *Adv. Polym. Sci.* **72** (1985) 1.
5. E. MOREL, V. BELLENGER and J. VERDU, *J. Mater. Sci.* **24** (1989) 69.
6. J. F. GERARD, J. GALY, J. P. PASCAULT, S. CUKIERMAN and J. L. HALARY, *Poly. Eng. Sci.* **31** (1991) 615.
7. E. ESUCHE, J. GALY, J. F. GERARD, J. P. PASCAULT and H. SAUTEREAU. Invited Lecture, 12th Conference on Polymer Networks. Prague. 24–26 July 1994.
8. J. J. NUSSELDER and H. L. BOS, 12th Conference on Polymer Networks. Paper SL37, Prague. 24–26 July 1994.
9. J. D. LEMAY and E. N. KELLEY *Adv. Polym. Sci.* **78** (1986) 116.
10. S. WU, *Polym. Eng. Sci.* **32** (1992) 823.
11. *Idem J. Appl. Polym. Sci.* **46** (1992) 619.
12. K. DUSEK, M. BLEHA and S. LUNAK, *J. Poly. Sci. Polym. Chem.* **15** (1977) 2393.
13. W. FISCH and W. HOFMANN. a) *Plast. Technol.* **8** (1961) 7, b) *J. Appl. Chem.* **6** (1956) 429.
14. R. P. KAMBOUR *Polym. Comm.* **24** (1983) 292.
15. L. C. E. STRUIK. "Physical ageing of amorphous polymers and other materials" (Elsevier, Amsterdam, 1978).
16. F. BUECHE, B. J. KINZIG and C. J. VOEN, *Polym. Lett.* **3** (1965) 399.
17. R. F. LANDEL and R. F. FEDORS in "Mechanical behaviour of Polymers". *Soc. Mater. Sci. Japan* (Kyoto), **3** (1972) 496.
18. J. E. MARK, *Adv. Polym. Sci.* **44** (1982) 1.

Received 12 October 1994
and accepted 20 November 1995